

# Applications of Particle-in-Cell Simulations to Fast Ion Slowing-Down

Elijah Kolmes

PEI Intern at the Princeton Plasma Physics Laboratory

Advised by Professor Samuel Cohen

November 1, 2014

## Abstract

I investigated fast ion slowing-down using the LSP particle simulation code with the goal of studying the slowing-down rates of very high-energy ions in a background plasma, with and without magnetic fields. In the simulations, I inserted fast ions as a homogeneous and isotropic plasma. I encountered and studied a couple of issues involving the LSP simulation code. I am especially interested in the physical implications of LSP's use of "clumped" macro-particles, and I have tested and analyzed the effects of macro-particle clumping on the physical behavior of these systems.

## 1 Introduction

In addition to its intrinsic interest as a basic characteristic of the behavior of plasmas, the rate at which fast ions slow down in a background plasma has a number of practical applications. In the context of a magnetic confinement device, fast ion slowing-down is relevant to the study of heating schemes (such as neutral beam injection and RF heating) that produce a number of very high-energy particles in a cooler plasma. However, this study has focused on a different application: understanding the behavior of high-energy fusion products. In the context of a field-reversed configuration, the slowing-down rates of fusion products are important to the problems of power and particle control. Essentially, I would like to understand where and how quickly hot fusion products will deposit their energy.

Rates of fast ion slowing-down are actually quite well-understood under certain conditions. This study is intended to explore areas of the plasma parameter space that are less well-studied and that are particularly relevant to the plasma in an FRC. In particular, I am interested in cases where the magnitude of the fast ion velocity  $v_f$  exceeds that of the thermal electron velocity  $v_e$ , and I am interested in cases in

which the ambient magnetic field is strong enough that one or more species' gyroradii  $\rho_L$  are less than the Debye length  $\lambda_D$ , because one might expect that to change the slowing-down rate.

## 2 Computational Concerns

### 2.1 LSP and Particle-in-Cell Codes

To study this problem, I used a particle simulation code called LSP. LSP is a particle-in-cell code. Generally speaking, that means that the code discretizes certain quantities and only tracks them on a finite number of lattice points.<sup>[1]</sup> This allows the code to track things like charge densities at many fewer individual points. The algorithm further simplifies the system by “clumping” together particles into larger macro-particles. For instance, if there are ten identical particles that are very close together, the code might instead consider a single macro-particle with ten times the charge, ten times the mass, ten times the energy, and so on. Some of the details of LSP's algorithm have important implications for this study.

### 2.2 Cell Size and Self-Heating

LSP allows the user to control the cell size of this discrete lattice. In order to minimize running time, I would like to minimize the number of lattice points that I have to keep track of, so it is preferable to use cell sizes that are as large as possible. However, there is a limit to how large the cells can be before the simulation will stop behaving itself. In particular, if the cell size  $\Delta x$  exceeds  $\lambda_D$ , there is a risk of encountering a nonphysical self-heating effect in which particles will appear to gain energy from nowhere. There are configurations of the LSP algorithm that can avoid this effect even for large  $\Delta x$ , but in this study I have elected to keep  $\Delta x \leq \lambda_D/7$ . This way, I have the freedom to change the settings of the algorithm without having to worry about self-heating. Because  $\lambda_D \propto \sqrt{T/n}$ , higher-density and lower-temperature plasmas are more computationally demanding to simulate.

### 2.3 Macro-Particles and Clumping

One part of the algorithm that is very important to its physical behavior is its use of macro-particles. If  $\zeta$  particles of a species are being lumped together for each macro-particle, that transforms the charge  $Z$ , mass  $m$ , temperature  $T$ , and density  $n$  of the

particles in the species as follows:

$$\begin{aligned} Z &\rightarrow \zeta Z \\ m &\rightarrow \zeta m \\ T &\rightarrow \zeta T \\ n &\rightarrow n/\zeta \end{aligned}$$

Most of these substitutions are intuitively clear. However, it may be worth mentioning that the temperature substitution is justified because the macro-particle inherits the combined energies of its constituents, and kinetic energy is proportional to  $T$ .<sup>[4]</sup>

Many of the physical quantities that are most important to the behavior of a plasma are preserved by this transformation, including the Debye length, gyrofrequency, plasma frequency, thermal velocity, and the ratio  $\beta$  of plasma pressure to magnetic pressure.<sup>[3]</sup> However, some physical parameters — including the slowing-down rate of fast ions — are not preserved by this transformation. I deal with this issue more fully in Section 3.5.

## 2.4 Collision Flags

One issue that has given me some trouble is the settings within LSP that govern particle collisions. In the LSP code, it is necessary to decide whether or not to manually turn on collisions for the different particle species. When the collision flags are on, LSP automatically simulates the expected results of interactions between distributions of particles within each cell. The details of how this is implemented are described in [6].

I have heard somewhat different advice from different experts (Dr. Adam Sefkow and Dr. Dale Welch) as to whether or not the collision flags should be turned on in simulations like ours. For most LSP simulations, the collision flags are necessary for the code to be able to simulate collisional behavior, and turning on the flags would not change the simulation if they were not needed. However, my simulations are unusual in that they resolve the Debye length — the side length of a cell never exceeds  $\lambda_D/7$ . Correctly simulating collisional behavior while using very small cell sizes is a little bit more complicated. Dr. Welch has warned that when using sufficiently small cell sizes, the collision flags are undesirable and can introduce artificial over-counting effects.

If the cell sizes were fine enough that these simulations were actually resolving the inter-particle spacing (which varies depending on the density being used, but which will be far smaller than a Debye length), then the situation would be more straightforward. It would no longer make sense to think of the contents of each cell as being thermal distributions of particles, and the important physics would all be in the interactions between cells, so there would be no need for collision flags, and any effects introduced by those settings that were intended to account for collisions within each cell would be non-physical. However, in these simulations, we are resolving  $\lambda_D$  but

we are not resolving the inter-particle spacing. This means that important collisional interactions could potentially be taking place both within and between cells. It is unclear exactly how fine the cell resolution has to be before the effects introduced by the collision flags are no longer physical.

I ran a variety of simulations with and without the collision flags, and the results suggested in a couple of ways that our simulations should have the collision flags turned off. For one thing, the scaling of the fast ion slowing-down rate with fast ion charge  $Z$  was very strange when I turned on the collision flags; with no flags, there was energy loss proportional to  $Z^2$ , but with the flags on the scaling was apparently exponential in  $Z$ . This did not seem physically reasonable. I also found that without the collision flags, the energy lost by the fast ions was very closely matched by energy gained by the background electrons. When the collision flags were turned on, this was no longer the case; in these runs, energy lost by the fast ions was often unaccounted for. When we turned on the collision flags, the slowing-down rate always increased. For higher-density runs (with electron number density at  $10^{11}$  per cc), the runs with the collision flags on were faster by a factor of about two. For the lower-density runs (electron number density at  $10^{10}$  per cc) the increase was often larger, although typically within a factor of ten. This means that even if I have made the wrong decision about the collision flags settings, my results should produce a lower bound for the slowing-down rate.

## 2.5 Energy Conservation

The nature of the particle-pushing algorithms that can be used in this kind of code is such that you can conserve energy or you can conserve momentum, but you cannot conserve both.<sup>[1]</sup> I chose to use an energy-conserving algorithm, but that doesn't necessarily mean that the energy conservation is perfect. This is, after all, a digital system, so given the very large number of interactions being simulated, I would like to make sure that I do not have to worry about rounding errors or any other numerical effects.

Before I started to try to simulate the actual slowing-down times of the fast ions, I spent a significant amount of time simulating background plasmas of protons and electrons on their own in order to measure the precision with which the algorithm conserves energy. These measurements matter because I would later be looking at very small variations in the fast ion energy; I needed to be sure that any energy loss that I observed was actually physical rather than some numerical artifact.

These measurements were taken with simulated plasmas containing equal numbers of electrons and protons. Over the time scales measured, there was not significant energy transfer between the two particle species. I tested a variety of number densities and a variety of electron temperatures; the cold protons were always left at 1 eV. Tests with varying electron temperatures are shown in Figure 1; tests with varying plasma densities are shown in Figure 2. The electrons always had a higher temperature, but

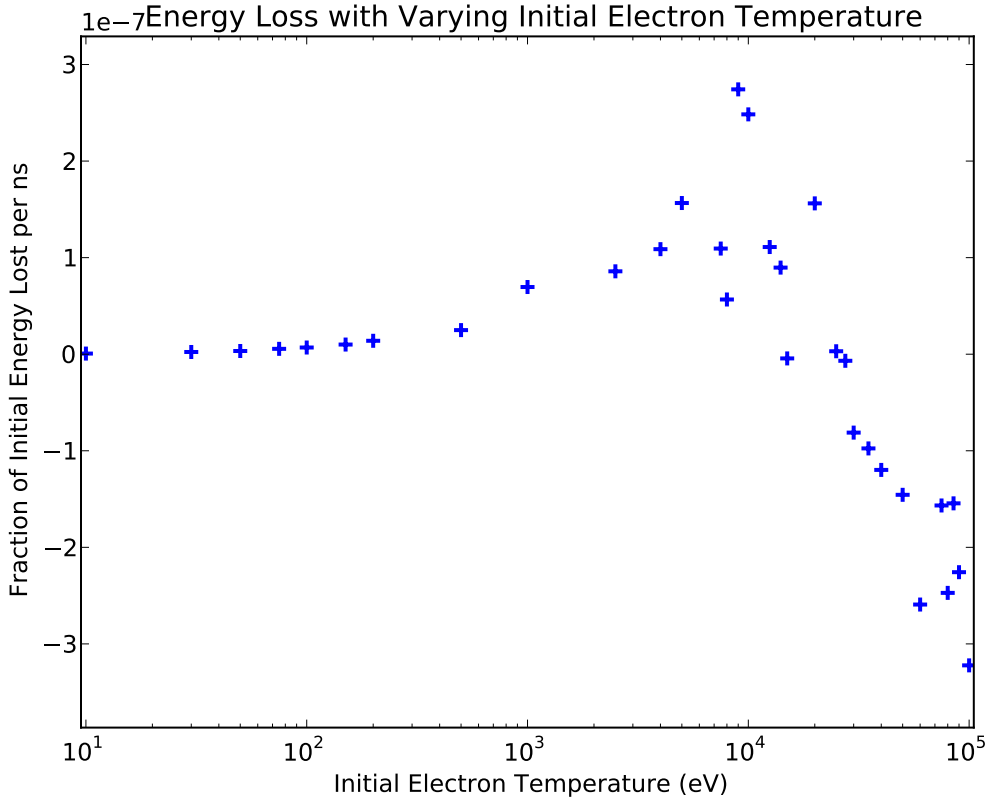


Figure 1: The fraction of initial energy not accounted for, per nanosecond. In all of these runs, the number densities of ions and electrons are both  $10^{11}$  per cc. The ion temperature is fixed at 1 eV.

there was no significant energy transfer between the two particle species. When not noted otherwise, these simulations used 0.5 cm by 0.5 cm two-dimensional boxes of plasma with periodic boundary conditions.

When I varied number density, I left the electron temperature at 100 eV. I tested number densities (always held equal for the two species) between  $10^{10}$  and  $10^{13}$  particles per cubic centimeter.

In the regimes that I am interested in (with electron temperatures on the order of 100 eV and number densities not exceeding  $10^{12}$  per  $\text{cm}^3$ ) the energy conservation is good at least to a part in  $10^7$  per nanosecond, and is often good to something more like a part in  $10^8$ . The energy conservation behavior at higher energies shows some unexpected behavior, with energy loss rates peaking at about 9 keV and then abruptly dropping. It is possible that this has to do with the size of the system and the way in which the Debye length scales with temperature. The system has a side

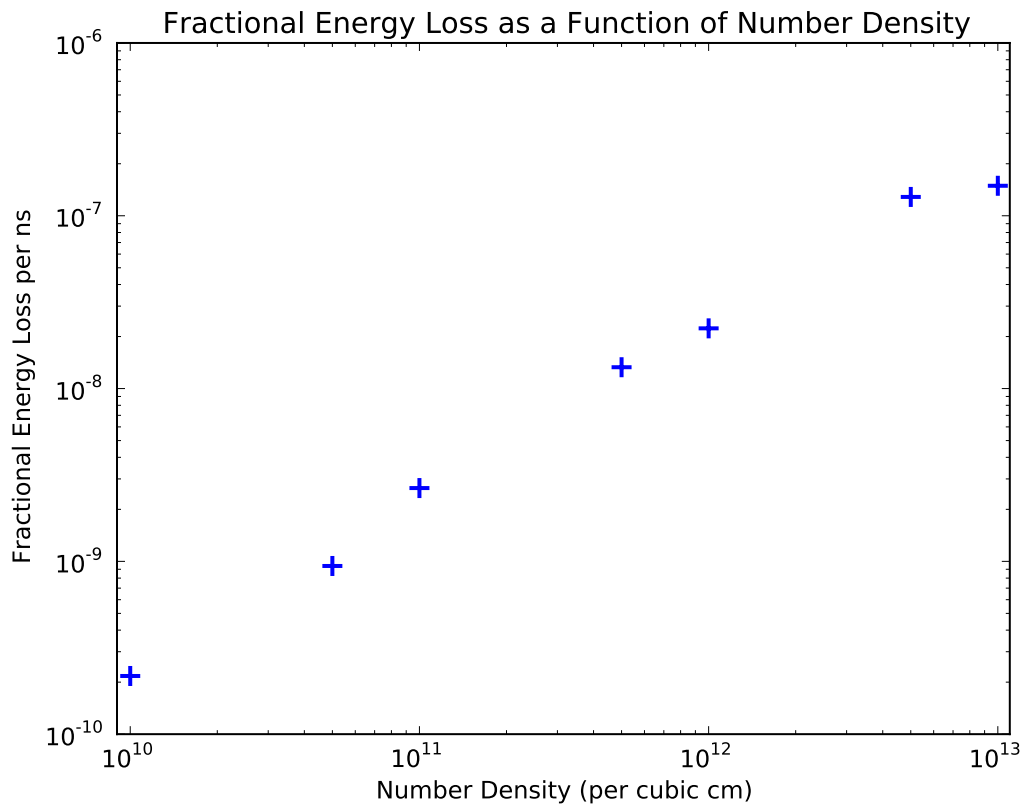


Figure 2: Fraction of the initial energy not accounted for, per nanosecond. The number densities of ions and electrons were held equal. The electron temperature is 100 eV and the ion temperature is 1 eV.

length of 0.5 cm, and the Debye length first exceeds one half of the system size at about the electron temperature of the peak (actually at just over 11 keV).

## 3 Theory of Fast Ion Slowing-Down

### 3.1 The Classical Result

Goldston and Rutherford derive the result that the rate of fast ion slowing-down in a plasma due to Coulomb collisions is given<sup>[2]</sup> by

$$\frac{dW}{dt} = -\frac{Z^2 e^4 \log \Lambda}{2^{1/2} \pi \epsilon_0^2} \left( \frac{n_e m_e^{1/2} W}{3\pi^{1/2} m T_e^{3/2}} + \frac{m^{1/2}}{4W^{1/2}} \sum_i \frac{n_i Z_i^2}{m_i} \right).$$

Here, quantities presented without a subscript correspond to the fast ions, those with the subscript  $e$  correspond to electrons, and the parameters of the thermal background ions are indexed by  $i$  (the sum allows for the case in which there are multiple species).  $\log \Lambda$  is typically about 20 for most plasmas; it is called the Coulomb logarithm, and it is discussed in Section 3.3. This result does not take into account other possible factors, such as instabilities in the plasma.

In the expression for  $dW/dt$ , the term due to interactions in background electrons goes like  $W$  and the term due to interactions with background ions goes like  $W^{-1/2}$ . Because of this, either the slowing term due to the ions or the term due to electrons will usually dominate. As the fast ions get more energetic, the electron term gets more important and the background ion term diminishes. I define the critical energy  $W_{\text{crit}}$  as the fast ion energy at which the electron and ion slowing-down terms are equal. A little bit of algebra gives us

$$W_{\text{crit}} = \left( \frac{3}{4n_e} \sqrt{\frac{\pi m^3 T_e^3}{m_e}} \sum_i \frac{n_i Z_i^2}{m_i} \right)^{2/3}$$

If  $W$  is significantly larger than  $W_{\text{crit}}$ , we can ignore the background ion slowing term. Conversely, if  $W$  is significantly smaller than  $W_{\text{crit}}$ , we can ignore the electron term.

### 3.2 High- and Low-Energy Regimes

If we have either  $W \gg W_{\text{crit}}$  or  $W \ll W_{\text{crit}}$ , then we can simplify the our slowing-down equation to get

$$\frac{dW}{dt} = \begin{cases} -\frac{Z^2 e^4 n_e m_e^{1/2} \log \Lambda}{m \epsilon_0^2 \sqrt{18\pi^3 T_e^3}} W & : W \gg W_{\text{crit}} \\ -\frac{Z^2 e^4 \log \Lambda}{4\pi \epsilon_0^2} \sqrt{\frac{m}{2W}} \sum_i \frac{n_i Z_i^2}{m_i} & : W \ll W_{\text{crit}} \end{cases}$$

This allows us to explicitly solve for  $W(t)$  in the high- and low-energy regimes.

$$W(t) = \begin{cases} W(0) \exp\left(-\frac{Z^2 e^4 n_e m_e^{1/2} \log \Lambda}{m \epsilon_0^2 \sqrt{18\pi^3 T_e^3}} t\right) & : W \gg W_{\text{crit}} \\ \left(W(0)^{3/2} - \frac{3Z^2 e^4 \log \Lambda}{8\pi \epsilon_0^2} \sqrt{\frac{m}{2}} \sum_i \frac{n_i Z_i^2}{m_i} t\right)^{2/3} & : W \ll W_{\text{crit}} \end{cases}$$

In fact, it is possible to get a general solution for  $W(t)$ , but the result is sufficiently unpleasant that I will omit it here.

For the purposes of understanding the behavior of fusion products in an FRC, I am mainly interested in the case in which the fast ion energy  $W \gg W_{\text{crit}}$ . In the above expressions,  $W$  refers to the energy of an individual fast ion particle rather than to the combined energies of all fast ions in the system. However, for the high-energy regime, the expressions for  $dW/dt$  and  $W(t)$  are linear in energy, so they describe the decay of the total energy  $W_{\text{tot}}$  of all fast ions in the system just as well. If this is written as  $W(t) = W(0) \exp(-t/t_s)$ , the characteristic decay time  $t_s$  will be the same whether  $W$  refers to the energy of an individual fast ion or the energy of all fast ions in the system. Because of this, it is often convenient to present our results as measurements of a decay constant  $\alpha = 1/t_s$ , where the theory predicts that for  $W \gg W_{\text{crit}}$ ,

$$\begin{aligned} \frac{dW}{dt} &= W(0) \exp(-\alpha t) \\ \alpha &= \frac{Z^2 e^4 n_e m_e^{1/2} \log \Lambda}{m \epsilon_0^2 \sqrt{18\pi^3 T_e^3}} \end{aligned}$$

The same is not true of the low-energy regime, in which  $dW/dt \propto W^{-1/2}$ .

When discussing the ‘‘characteristic’’ slowing-down time  $t_s$ , it is important to remember that  $t_s$  is not the total amount of time required for a fast particle to slow to thermal velocities. Rather, it is the amount of time that it takes for the particle’s energy to be reduced by a factor of  $e$  in the high-energy regime. In fact, it is also possible to compute the total expected time for a fast ion to slow to thermal velocities. This total time  $\tau$  is given<sup>[5]</sup> by

$$\tau = \frac{t_s}{3} \log \left[ 1 + \left( \frac{W}{W_{\text{crit}}} \right)^{3/2} \right].$$

### 3.3 The Coulomb Logarithm

The Coulomb logarithm  $\log \Lambda$  is a parameter which introduces a certain amount of uncertainty into any calculations of  $dW/dt$ . The Coulomb logarithm shows up in our expression for  $dW/dt$  because of its relationship with Coulomb collisions.

If I try to derive  $dW/dt$  by thinking about energy losses from Coulomb collisions (an exercise that I won't go through here but which is presented nicely<sup>[2]</sup> by Goldston and Rutherford), it turns out that the rate of energy loss diverges unless I assume that there is some maximal range beyond which Coulomb collisions are not important. More specifically, I need to put an upper bound on the impact parameter, which is the distance of closest approach of the unperturbed particle trajectories. Happily, this makes good physical sense, because Debye shielding should prevent very long-range interactions between particles in the plasma. In the resulting calculation, a term emerges that depends logarithmically on a parameter (which we call  $\Lambda$ ) that is defined as the ratio of the maximal impact parameter and the impact parameter associated with right-angle scattering. The problem is that there isn't an immediately obvious way of computing  $\Lambda$ , since there is no nice way of computing that maximal impact parameter (except that it should look more or less like the Debye length).

Different sources give different estimates for  $\Lambda$  and  $\log \Lambda$ . The NRL plasma formulary<sup>[3]</sup> states that for interactions between electrons and ions,

$$\log \Lambda = \begin{cases} 23 - \log(n_e^{1/2} Z T_e^{3/2}) & : T_i m_e / m_i < T_e < 10 Z^2 \text{ eV} \\ 24 - \log(n_e^{1/2} T_e^{-1}) & : T_i m_e / m_i < 10 Z^2 \text{ eV} < T_e \\ 30 - \log(n_i^{1/2} T_i^{-3/2} Z^2 \mu^{-1}) & : T_e < T_i Z m_e / m_i. \end{cases}$$

Here  $\mu$  is the mass of the fast ion in units as a multiple of the mass of a proton. In my calculations, I will use the NRL results, since they are the most detailed that I have found. However, Goldston and Rutherford<sup>[2]</sup> instead give that  $\Lambda \sim (12\pi/Z) n_e \lambda_D^2 \sim 3T/Z e^2$ . This scaling is not fully consistent with the NRL results for any of the three regimes listed. Other sources give slightly different results. This suggests that any estimate I make for  $\Lambda$  introduces a certain amount of uncertainty into the results for quantities like  $dW/dt$ . The NRL formulary itself suggests that its own results for  $\log \Lambda$  will only be good to within about ten percent. Fortunately,  $dW/dt$  scales with  $\log \Lambda$  rather than with  $\Lambda$  itself, so we can tolerate a certain amount of uncertainty in  $\Lambda$ . As Goldston and Rutherford point out,  $\log \Lambda$  stays within a factor of two even for very large changes in the characteristics of the plasma. As such, I can expect estimates of  $\log \Lambda$  to introduce some error into our calculations, but even a catastrophically bad estimate should not be responsible for more than perhaps a factor of two in the slowing-down rate. If there are discrepancies larger than that between our predictions and our simulations, we must look elsewhere for the culprit.

### 3.4 Complications in an FRC-like Plasma

The plasmas found in a field-reversed configuration have two particularly important characteristics that make them unusual. The first is that  $v_f > v_e$ ; that is, the plasma contains fast ions that have such high energies that they actually move more quickly than the thermal electrons, despite the large difference in mass. For instance, one of the products of D-<sup>3</sup>He fusion is 14.7 MeV protons. These protons may be about

1800 times more massive than the electrons in the plasma, but if the electrons have energies the range of hundreds of electron-volts, the energy difference is a factor of order  $10^5$ , and the fast ions will have larger velocities. Ordinarily — i.e., for a plasma in which the difference particle species have similar energies — I would expect ion velocities to be far smaller than electron velocities, so the ions can react only very sluggishly to motion of the electrons. Therefore, the basic behavior of a plasma like the ones studied here may exhibit unconventional behavior.

Another important characteristic of an FRC-like plasma is the very large magnetic field. FRCs are very high- $\beta$  devices, and the magnetic fields can be strong enough that a particle’s gyroradius  $\rho_L$  can be smaller than the Debye length. In the regime where  $\rho_L < \lambda_D$ , it is possible that the magnetic field can have such a large effect on individual particle orbits that it actually disrupts the shielding behavior of the plasma.

### 3.5 Predicted Corrections Due to Particle “Clumping”

In the high-energy regime where  $W \gg W_{\text{crit}}$ , the coefficient  $\alpha$  of the exponential decay had the dependence  $\alpha \propto Z^2 n_e m_e^{1/2} / m T^{3/2}$ . When particles are grouped together to form macro-particles, the quantity  $\alpha$  is not preserved; if each fast ion macro-particle represents  $\zeta_f$  real ions and each electron macro-particle represents  $\zeta_e$  real electrons, then we can compute the dependence of the slowing-down rate on  $\zeta_e$ ,  $\zeta_i$ , and  $\zeta_f$ . If I simply apply the prescription from Section 2.3 directly to our earlier results (sending  $Z \rightarrow \zeta Z$ ,  $m \rightarrow \zeta m$ , and so forth), I should expect  $\alpha \propto \zeta_f / \zeta_e^2$  and  $t_s \propto \zeta_e^2 / \zeta_f$ . However, this result is not quite right. My results from the previous section all assume that each electron has charge  $e$ ; there are no  $Z_e^2$  terms in those equations because in a physical system, we always expect  $Z_e^2 = 1$ . If I had kept those terms instead of setting them equal to one, I would have found that

$$\frac{dW}{dt} = -\frac{Z^2 e^4 \log \Lambda}{2^{1/2} \pi \epsilon_0^2} \left( \frac{n_e Z_e^2 m_e^{1/2} W}{3\pi^{1/2} m T_e^{3/2}} + \frac{m^{1/2}}{4W^{1/2}} \sum_i \frac{n_i Z_i^2}{m_i} \right).$$

With the inclusion of the additional  $Z_e^2$  term, we instead find that  $\alpha \propto \zeta_f$ , with no explicit dependence on  $\zeta_e$ .

In the low-energy regime in which  $W \ll W_{\text{crit}}$ , instead  $dW/dt \propto \zeta_f^2$ . Then the fractional rate of energy loss goes like  $(dW/dt)/W(0) \propto \zeta_f$ . Even in this regime, where interactions with background ions are important, the number of background ions per macro-particle does not directly affect the results.

The quantities  $\zeta_e$  and  $\zeta_f$  are both straightforward to compute, so it might initially seem like it should be easy to recover physically “correct” results from our simulations simply by removing a factor of  $\zeta_f$ . However, there are still a few things to be careful of. The first thing that needs to be checked is the critical energy. The solution  $W(t) = W(0) \exp(-\alpha t)$  is only valid when  $W$  is significantly larger than  $W_{\text{crit}}$ , and

in fact,  $W_{\text{crit}}$  is itself not preserved by particle clumping. It turns out that  $W_{\text{crit}} \propto \zeta_f$ . However, this expression may be slightly misleading, since the energy per macro-particle will also scale with  $\zeta_f$ . The above expression describes the critical energy of a simulated macro-particle; the effective critical energy for the fast ions before clumping would not depend on  $\zeta_f$ , since the energy per macro-particle goes up by the same factor that  $W_{\text{crit}}$  does. Therefore, if the “real,” physical parameters of a system place it well within a regime where I can ignore the slowing due to thermal ions, the version of that system simulated in LSP should still have  $W \gg W_{\text{crit}}$ .

There are a couple of additional effects that might further complicate this picture, and not all of them resolve themselves so cleanly. Macro-particle clumping changes a couple of other parameters of the system, including the average separation between two particles and the rate of inter-particle collisions. The slowing-down rate does not explicitly depend on either of these quantities, but they might still be important. LSP discretizes both time and space; if the collision rate changes, that could conceivably change whether or not the time step size is adequate, and if the inter-particle separation changes but the spatial cell size does not, the algorithm might behave differently.

Another possible effect involves the relative masses of different particles. Physically, the electrons should be much less massive than the fast ions. This has significant consequences for the tendency of the particles to transfer energy and momentum.<sup>[2]</sup> However, if the particles are clumped into macro-particles in such a way that  $\zeta_e \gg \zeta_f$ , it could be that the electron *macro-particles* are no longer much less massive than their fast ion counterparts. This would make the previous predictions for  $dW/dt$  inaccurate.

## 4 Measurements of Slowing-Down Times

### 4.1 Overall Approach

Some of my earlier efforts at measuring the slowing-down times involved injecting a beam of fast ions into a homogeneous background plasma of protons and electrons. However, for most of my simulations, I used a different approach, and instead inserted the fast ions with homogeneous position and velocity distributions. The latter approach has a couple of different advantages. First, it allows me to avoid instabilities like the two-stream instability that can arise in different configurations (such as a directed beam of fast ions). Second, it may more accurately reflect the conditions inside an FRC, since the high-energy fusion products will not naturally move in any particular direction and will be spread relatively evenly throughout a region of plasma.

## 4.2 Tests of Particle Clumping Effects

In order to investigate the quantitative effects of macro-particle clumping, I ran simulations with a variety of values of  $\zeta_e$  and  $\zeta_f$  (and otherwise identical physical parameters). In these simulations, I had  $n_e = n_i = 10^{11}$  per cc, and  $n_f = 10^8$  per cc. The fast ions started at  $10^7$  eV, the background ions started at 1 eV, and the electrons started at 100 eV. I increased the fast ion charge to 100 times that of a proton in order to increase the slowing-down rate. This was intended both to make  $dW/dt$  measurable in a shorter simulation and to make it easier to separate out the “overall” slowing-down rate from background fluctuations in the fast ion energy.

I simulated a two-dimensional box of plasma with a side length of 0.5 cm, divided into 22,500 cells each with a side length of 1/300 cm. When I varied  $\zeta_f$ , I maintained 256 electrons per cell and 64 background ions per cell — that is,  $\zeta_e \approx 4340$  and  $\zeta_i \approx 17361$ . Some of these results are shown in Figures 3 and 4. The fast ion energy has  $W(0) = 15$  MeV and  $W_{\text{crit}} = 1480$  eV, so we should be easily within the high-energy regime.

The experiment was designed to measure the decay coefficient  $\alpha$  for the high-energy regime. Since I was measuring very early times (typically under 30 ns),  $dW/dt$  is virtually constant during the simulated interval. Because of this, my measurements of a best-fit  $\alpha$  are functionally equivalent to measurements of the fractional energy loss rate  $(-dW/dt)/(W(0))$  at time  $t = 0$ . In both the high- and low-energy regimes,  $(-dW/dt)/(W(0)) \propto \zeta_f$ .

The results suggest that  $\alpha$  — that is,  $(-dW/dt)/(W(0))$  — is inversely proportional to the number of macro-particles per cell, so it follows that  $\alpha \propto \zeta_f$ . More precisely, I found that  $\alpha$  went like the number of discrete macro-particles per cell to the -0.95 power. This evidence is consistent with the predicted effects of fast ion macro-particle clumping on  $dW/dt$  in either regime. It is some of the best evidence available for the dependence of slowing-down rates on  $\zeta_f$ . However, it is not strong evidence one way or the other for the effects of fast ion macro-particle clumping on  $W_{\text{crit}}$ , since I would have expected the same results in either regime.

When I varied  $\zeta_e$ , I maintained 64 background ion and 64 fast ion macro-particles per cell.  $\zeta_e$  fell between 2,295 and 30,865. Some of these results are shown in Figure 5. This means that  $W_{\text{crit,eff}}$  varied between about  $4.4 \times 10^7$  and  $1.4 \times 10^9$  eV. In all of these cases,  $W \gg W_{\text{crit}}$ .

I observed that for small  $\zeta_e$ ,  $-dW/dt$  fluctuated and increased a little as the number of electron macro-particles per cell increased. The predictions from Section 3.5 suggest that  $-dW/dt$  should not depend at all on  $\zeta_e$ . However, as both Dr. Welch and Dr. Sefkow have pointed out, small macro-particle counts can cause statistical noise in LSP simulations. This could explain the variations in  $\alpha$  for small  $\zeta_e$ .

I also ran a few simulations with different number of background ion macro-particles per cell. Runs with different values for  $\zeta_{i,th}$  yielded identical results, to within the expected levels of error. This was unsurprising, since the slowing-down rate should not be sensitive to thermal ion clumping (whether or not  $W \gg W_{\text{crit}}$ ).

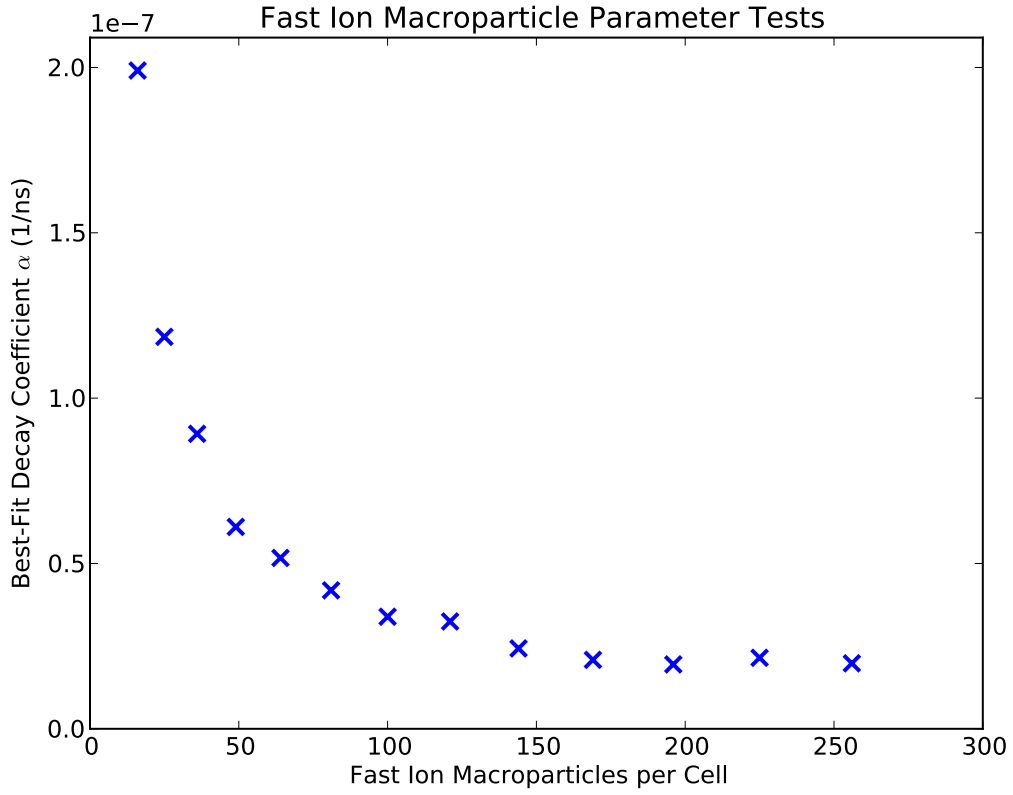


Figure 3: Tests of the fast ion slowing-down in which all physical parameters were held fixed and the number of fast ion macro-particles per cell was varied. Here  $n_e = n_i = 10^{11}$  per cc,  $n_f = 10^8$  per cc,  $T_e = 100$  eV,  $T_i = 1$  eV, and  $T_f = 10^7$  eV.

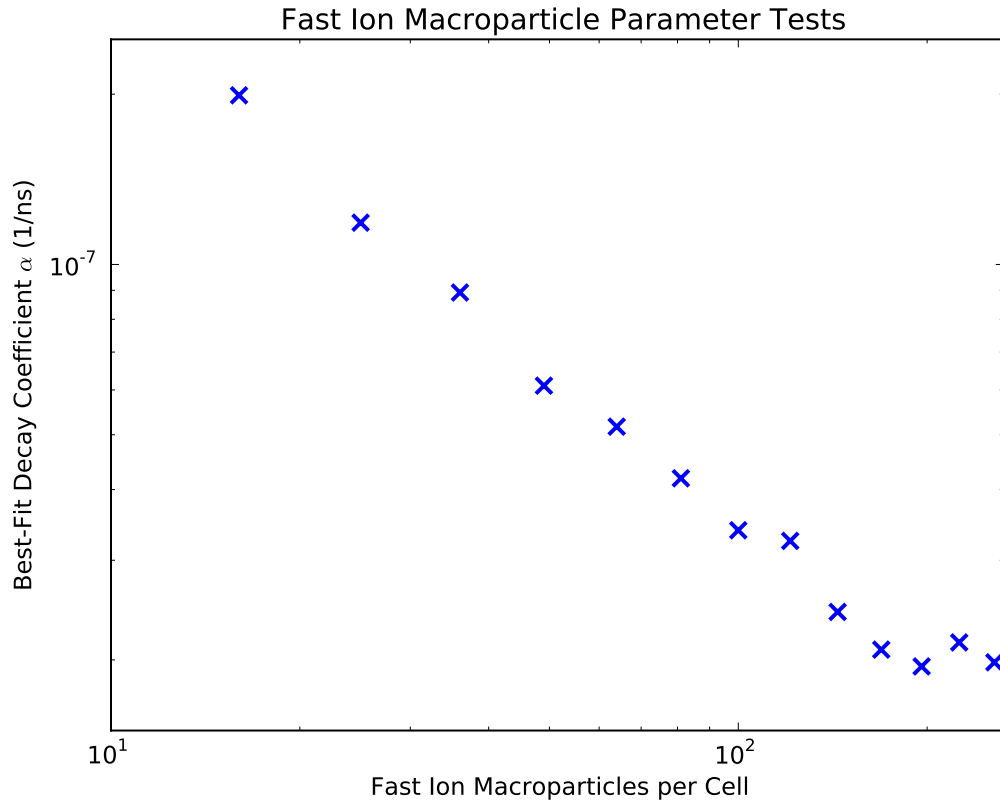


Figure 4: Tests of the fast ion slowing-down in which all physical parameters were held fixed and the number of fast ion macro-particles per cell was varied, presented on a log-log scale. As in Figure 3,  $n_e = n_i = 10^{11}$  per cc,  $n_f = 10^8$  per cc,  $T_e = 100$  eV,  $T_i = 1$  eV, and  $T_f = 10^7$  eV.

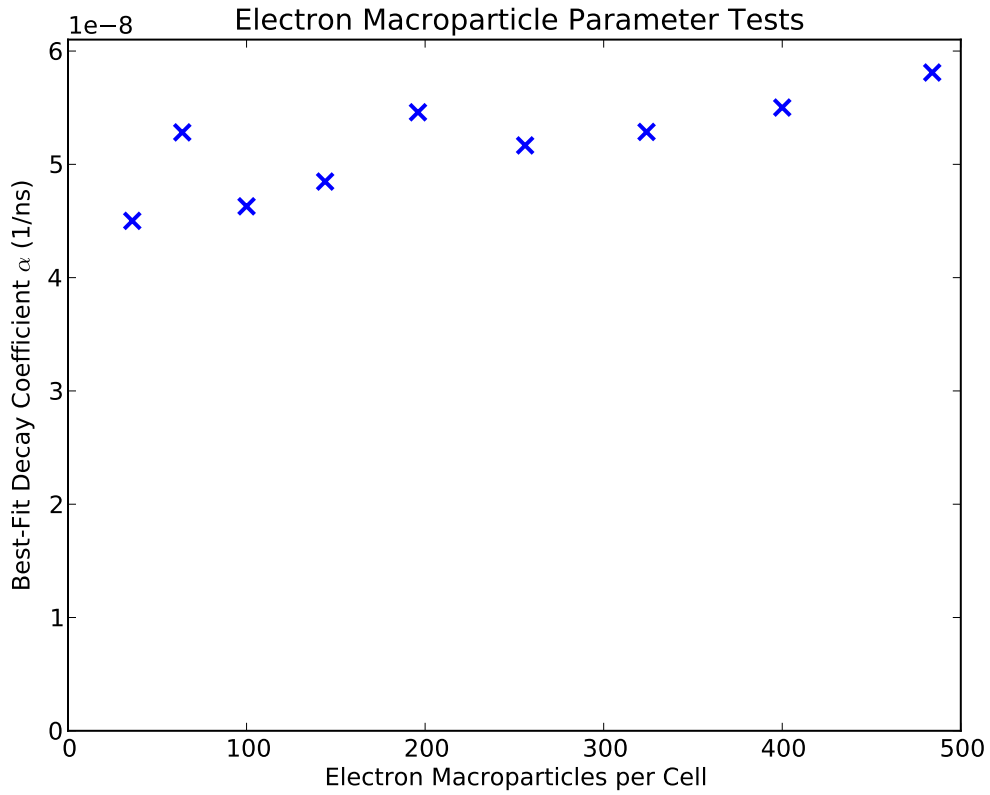


Figure 5: Tests of fast ion slowing-down in which all physical parameters were fixed and the number of electron macro-particles per cell was varied. Here, as before,  $n_e = n_i = 10^{11}$  per cc,  $n_f = 10^8$  per cc,  $T_e = 100$  eV,  $T_i = 1$  eV, and  $T_f = 10^7$  eV.

### 4.3 Early Simulations: Scaling with Charge

One of the largest data sets measuring the slowing-down rates addressed two different questions: how does  $\alpha$  scale with fast ion charge, and how does  $\alpha$  scale with plasma density? This attempt was only partially successful at answering these questions. I collected this data before I fully understood the implications of macro-particle clumping, so I chose (somewhat arbitrarily) to have 256 electron macro-particles, 256 thermal ion macro-particles, and 4 fast ion macro-particles per cell. When choosing the cell size, I tried to keep the length just under  $\lambda_D/7$ , so for  $n_e = 10^{10} \text{ cm}^{-3}$  I divided the system into 2,784 cells, for  $n_e = 10^{11} \text{ cm}^{-3}$  I used 22,500 cells, and for  $n_e = 10^{12} \text{ cm}^{-3}$  I used 221,841 cells. I always set the number density of the fast ions to  $n_f = n_e/100$ . Then, in order to maintain charge neutrality, I set the thermal ion density to  $n_{i,th} = (1 - Z/100)n_e$  — here, as before,  $Z$  is the charge of the fast ion in units of the charge of an electron.

The clearest result of these simulations (and the reason why I describe them here) is that, as the equations predict, the slowing-down rate is proportional to  $Z^2$ . The data set here demonstrates this dependence out to  $Z = 40$ ; the closest quadratic fit for each density is shown by the dotted line. In fact, the original data went out significantly farther (and the  $Z^2$  scaling appears to continue well past  $Z = 40$ ), but I present the results of these particular simulations because they were all set up the same way; other runs with higher  $Z$  used slightly different settings, for a variety of reasons.

The results for number density are more complicated. The best-fit curves for each of the densities are  $\alpha = 0.13 \text{ s}^{-1}$ ,  $\alpha = 0.80 \text{ s}^{-1}$ , and  $\alpha = 4.5 \text{ s}^{-1}$  for  $n_e = 10^{10}$  per cc,  $10^{11}$  per cc, and  $10^{12}$  per cc, respectively. This shows that  $\alpha$  increases by a factor of about six for every factor of ten increase in  $n_e$ .

In the high-energy regime, I would expect the slowing-down rate to be proportional to  $n_e$ . In the low-energy regime, I would expect the rate to be proportional to  $n_i$ , which in these simulations scales along with  $n_e$ . This simulations were firmly within the high-energy regime.

Additional clumping effects do introduce a small correction to the slowing-down rates at these different plasma densities. If I increase the densities by a factor of ten, I immediately increase  $\zeta_e$  and  $\zeta_f$  by a factor of ten each. However, even though the number of macro-particles per cell is fixed in all of these simulations, the number of cells is not; it goes up by a factor of 9.77 between  $n_e = 10^{10} \text{ cm}^{-3}$  and  $n_e = 10^{11} \text{ cm}^{-3}$ , then by a factor of 9.86 when  $n_e$  increases to  $10^{12} \text{ cm}^{-3}$ . In all, then, using  $\alpha \propto \zeta_f$ , in order to correct for the changing macro-particle settings I should reduce  $\alpha$  at  $n_e = 10^{11} \text{ cm}^{-3}$  by a factor of 1.024 and then at  $n_e = 10^{12} \text{ cm}^{-3}$  by an additional factor of 1.014. This is not enough to explain the unexpected behavior of  $\alpha$  with growing plasma density.

Even considering all of these additional corrections, the fact remains that the rate of fast ion energy loss simply does not increase as quickly as expected as the plasma density increases. I am not certain why this is true. One possibility, suggested

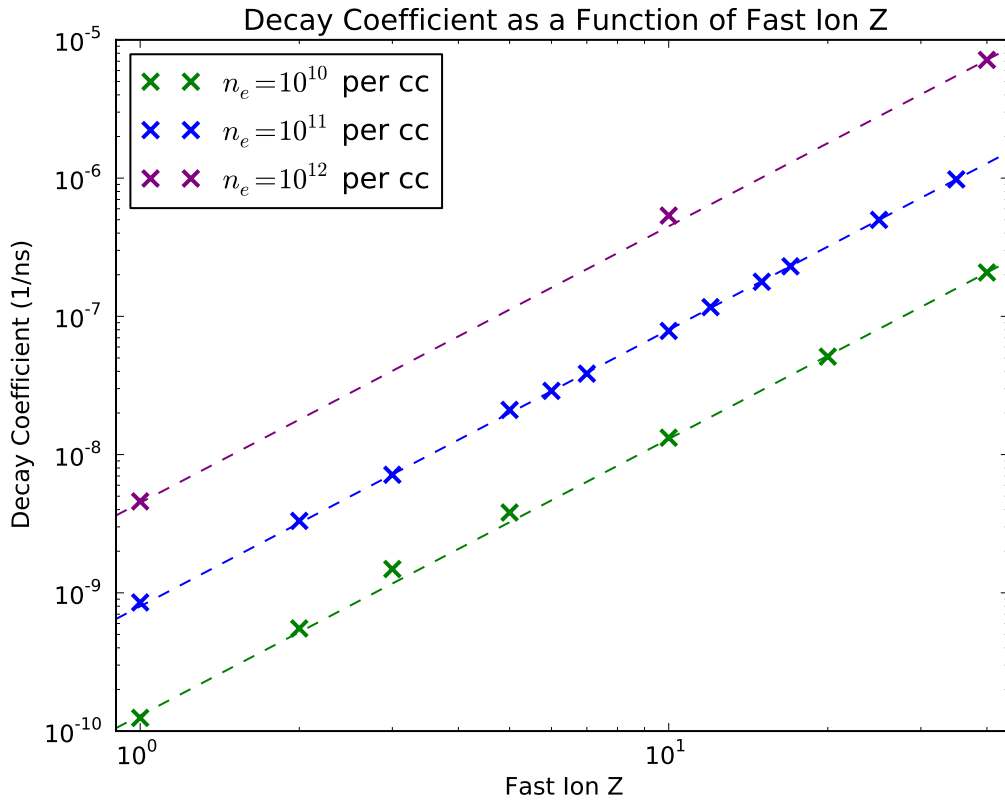


Figure 6: Slowing-down rate measured with varying background plasma density and varying fast ion charge. Here  $T_e = 100$  eV,  $T_i = 1$  eV, and  $T_f = 10^7$  eV.

by Dr. Sefkow, had to do with the differing time step intervals in these different simulations. In these simulations, I set the time steps so that they were ninety percent of the Courant limit, which is an upper limit for time steps above which the simulations are not stable. The Courant limit for a system is proportional to the cell size, so each increase in plasma density by a factor of ten was accompanied by a decrease in time step by a factor of about three. After speaking with Dr. Sefkow, I tried manually varying the time step on a series of similar, low-density runs (with  $n_e = n_i = 10^3 n_f = 10^{10} \text{ cm}^{-3}$ ). So long as I stayed under the Courant limit, I did not see any noticeable change in my results. However, I have not done the kind of comprehensive tests that I would need to be sure that differing time steps are not affecting my results, and I do not fully understand the conditions under which differing time steps can change the physical behavior of a simulation.

It is also true that the tests at different densities had different cell sizes, and it is possible that the differing spatial resolutions had some unforeseen effects on the behavior of the systems (this is another possibility that Dr. Sefkow suggested I should investigate). Again, basic tests on low-density systems have not shown any noticeable changes when I changed the spatial resolution, but it is still possible that there are conditions under which spatial resolution is important and I have not found them yet.

Another possibility, originally raised by Professor Cohen, is that it is a consequence of the fact that these simulations are two-dimensional. It might not be so surprising if a change as fundamental as the one between two and three dimensions could change the scaling of the plasma's behavior with a parameter as spatial as number density.

## 5 Conclusion

The effects of macro-particle clumping on the physical behavior of these systems has turned out to be far more important than initially anticipated, but I now have a better understanding of the LSP code. Going forward, there are a number of challenges to deal with in order to be able to simulate systems that have the physical behavior we want. The main one is the problem of collisions; it was never completely clear that the LSP code was handling particle collisions correctly with the settings used here. It is important that we gain a better understanding of the way in which LSP handles collisions.

The unexpectedly slow scaling of  $-dW/dt$  with number density is also potentially important. If  $-dW/dt$  is picking up a non-physical factor of 1.6 for every factor of ten in the background plasma number density, that would introduce very significant error into our measurements. It would be very interesting to see if this problem would disappear if we switched from two-dimensional to three-dimensional simulations.

However, if we can resolve both of these two main challenges, it may still be possible to get good measurements of fast ion slowing-down rates using LSP. The direct effects of the clumping factors  $\varsigma_e$ ,  $\varsigma_i$ , and  $\varsigma_f$  appear to be predictable enough

that we can hope to recover the “physical” slowing-down times simply by computing and applying the relevant correction terms (and that may be as simple as dividing  $-dW/dt$  by  $\zeta_f$ ) so long as we can control the secondary effects of macro-particle clumping described in Section 3.5.

## 6 Acknowledgements

I owe many thanks to Professor Samuel Cohen at PPPL, who offered guidance throughout this project and without whom this would not have been possible. I would also like to thank Dr. Dale Welch from Voss Scientific and Dr. Adam Sefkow from Sandia National Labs for their advice regarding the use of LSP.

This project was funded as an internship from the Princeton Environmental Institute. Many of these simulations were run on the computing cluster at PPPL. Some were run on the Edison cluster at the National Energy Research Scientific Computing Center, a DOE Office of Science User Facility supported by the Office of Science of the DOE under Contract No. DE-AC02-05CH11231.

# A Appendix: Code

## A.1 Sample Deck

This deck was one of a series in which I varied the number of macro-particles per cell for each of the different species. It is a relatively late deck, with no magnetic field.

```
;GLSP version 6.97 : GLSP_131122
;(07/15/2014 23:07:47)
;GLSP comments --BEGIN--
;GLSP comments --END--
;GLSP compiler flags --BEGIN--
; CAR_X_Y CHARGE_DENSITY DOUBLE_PRECISION EXTENDED_PARTICLES
; MAX_CHARGE_STATE=7 MAX_SPECIES=3 MULTI_PROCESS NUMBER_DENSITIES
; PRIMARY_SPECIES=2 UNITS_LSP
;GLSP compiler flags --END--
;GLSP metric: 0 dimensions: xy
[Control]
;Time-advance
  time_limit_ns 50
  time_step_ns 7E-5
;Parallel Processing
  balance_interval 10000
;(Diagnostic Output)
  probe_output_digits 12
;(Diagnostic Output) Flags
  dump_bfield_flag OFF
  dump_charge_density_flag ON
  dump_current_density_flag ON
  dump_number_densities_flag ON
  dump_rho_background_flag ON
  dump_time_zero_flag ON
;(Diagnostic Output) Dump Intervals
  dump_interval_ns 20000
  dump_steps
1000
end
  probe_interval 20
;(Diagnostic Output) Movie Controls
  field_movie_interval_ns 0.10
  scalar_movie_interval_ns 0.10
  scalar_movie_coordinate Z 0
  field_movie_components EX EY EZ
```

```

    scalar_movie_components charge_density number_densities
;Numerical Checks and Reports
    print_convergence_flag ON
;
[Grid]
;
grid1 ; grid 1
xmin 0.0
xmax 0.5
x-cells 150
;
ymin 0.0
ymax 0.5
y-cells 150
;
;
[Regions]
;
region1 ; region 1
;
grid 1
xmin 0.0
xmax 0.5
ymin 0.0
ymax 0.5
number_of_domains 32
split_direction XSPLIT
number_of_cells AUTO
;
;
[Boundaries]
;
periodic ; Periodic Y
from 0.0 0.0 0.0
to 0.5 0.5 1
normal Y
;
periodic ; Periodic X
from 0.0 0.0 0.0
to 0.5 0.5 1
normal X
;

```

```
[Particle Species]
species1 ; electrons
charge -1.0
mass 1.0
migrant_species_flag off
implicit_species_flag off
particle_motion_flag on
particle_forces_option PRIMARY
transverse_weighting_flag on
particle_kinematics_option STANDARD
scattering_flag off
selection_ratio 1.0
;
species2 ; protons
charge 1.0
mass 1836.153
atomic_number 1
migrant_species_flag off
implicit_species_flag off
particle_motion_flag on
particle_forces_option PRIMARY
transverse_weighting_flag on
particle_kinematics_option STANDARD
scattering_flag off
selection_ratio 1.0
;
species3 ; fast
charge 100.0
mass 1836.153
atomic_number 1
migrant_species_flag off
implicit_species_flag off
particle_motion_flag on
particle_forces_option PRIMARY
transverse_weighting_flag on
particle_kinematics_option STANDARD
scattering_flag off
selection_ratio 1.0
;
;
[Particle Creation]
;
```

```
plasma ; Initial electrons
from 0.0 0.0 0.0
to 0.5 0.5 0.0
species 1
movie_tag 1
unbound off
discrete_numbers 16 16 1
random off
multiple_number 1
cloud_radius 0.0
density_function 1
momentum_function 0
reference_point 0.0 0.0 0.0
density_flags 0 0 0
momentum_flags 0 0 0
drift_velocity 0 0 0
rotation off
thermal_energy 100
random_energy_function 0
spatial_function 0
movie_fraction 1.0
;
plasma ; Initial protons
from 0.0 0.0 0.0
to 0.5 0.5 0.0
species 2
movie_tag 2
unbound off
discrete_numbers 8 8 1
random off
multiple_number 1
cloud_radius 0.0
density_function 1
momentum_function 0
reference_point 0.0 0.0 0.0
density_flags 0 0 0
momentum_flags 0 0 0
drift_velocity 0 0 0
rotation off
thermal_energy 1
random_energy_function 0
spatial_function 0
```

```

movie_fraction 1.0
;
plasma ; Fast ions
from 0.0 0.0 0.0
to 0.5 0.5 0.0
species 3
movie_tag 3
unbound off
discrete_numbers 8 8 1
random off
multiple_number 1
cloud_radius 0.0
density_function 2
momentum_function 0
reference_point 0.0 0.0 0.0
density_flags 0 0 0
momentum_flags 0 0 0
drift_velocity 0 0 0
rotation off
thermal_energy 10000000
random_energy_function 0
spatial_function 0
movie_fraction 1.0
;
;
[Functions]
function1 ; Initial density
type 1
coefficients 1E11 end
;
function2 ; Fast ion density
type 1
coefficients 1E8 end
;
;
[Probes]
;
probe1 ; number1
global number species 1
;
probe2 ; number2
global number species 2

```

```
;
probe3 ; total_energy
energy total_energy
;
probe4 ; particle_energy
energy particle_energy
;
probe5 ; ketot1
global ketot species 1
;
probe6 ; ketot2
global ketot species 2
;
probe7 ; net_energy
energy net_energy
;
probe8 ; vxtot1
global vxtot species 1
;
probe9 ; vxtot2
global vxtot species 2
;
probe10 ; vytot1
global vytot species 1
;
probe11 ; vytot2
global vytot species 2
;
probe12 ;
energy field_energy
;
probe13 ; number3
global number species 3
;
probe14 ; vxtot3
global vxtot species 3
;
probe15 ; vytot3
global vytot species 3
;
probe16 ; ketot3
global ketot species 3
```

;

## References

- [1] C. K. Birdsall and A. B. Langdon, Plasma Physics via Computer Simulation, 1st ed. (McGraw-Hill Book Company, New York, NY 1985), pp. 20-22, 288-301.
- [2] R. J. Goldston and P. H. Rutherford, Introduction to Plasma Physics, 1st ed. (Institute of Physics Publishing, Philadelphia, PA 2003), pp. 165-170, 229-239.
- [3] J. D. Huba, *NRL Plasma Formulary*, (Naval Research Laboratory, Washington, DC 2009), pp. 28-29, 34-35.
- [4] Charles Kittel and Herbert Kroemer, Thermal Physics, 2nd ed. (W.H. Freeman and Company, New York, NY 1980), pp. 89-116.
- [5] Thomas H. Stix, *Heating of Toroidal Plasmas by Neutral Injection*, Plasma Phys. **14**, 367 (1972).
- [6] D. R. Welch, D. V. Rose, *et al.*, *Integrated Simulation of the Generation and Transport of Proton Beams from Laser-Target Interaction*, Phys. Plasmas **13**, 063105 (2006).